Defect reduction in $(11\bar{2}0)$ a-plane GaN by two-stage epitaxial lateral overgrowth

X. Ni[*a], Ü. Özgür[a], Y. Fu[a], N. Biyikli[a], J. Xie[a], A. A. Baski[b], and H. Morkoç[a,b]

[a]*Department of Electrical and Computer Engineering, Virginia Commonwealth University, Richmond, Virginia 23284*

[b]*Department of Physics, Virginia Commonwealth University, Richmond, Virginia 23284*

Z. Liliental-Weber

Lawrence Berkeley National Laboratory, Berkeley, California 94720

Abstract

In the epitaxial lateral overgrowth (ELO) of $(11\bar{2}0)$ a-plane GaN, the uneven growth rates of two opposing wings, Ga- and N-wings, makes the coalescence of two neighboring wings more difficult than that in c-plane GaN. We report a two-stage growth method to get uniformly coalesced epitaxial lateral overgrown a-plane GaN using metalorganic chemical vapor deposition (MOCVD) by employing relatively lower growth temperature in the first step followed by enhanced lateral growth in the second. Using this method, the height differences between Ga-polar and N-polar wings at the coalescence front could be reduced, thereby making the coalescence of two wings much easier. Transmission electron microscopy (TEM) showed that the threading dislocation density in the wing areas was 1.0×10^{8}cm^{-2}, more than two orders of magnitude lower than that in the window areas (4.2×10^{10}cm^{-2}). However, high density of basal stacking faults of 1.2×10^{4} cm^{-1} was still observed in the wing areas as compared to c-plane GaN. Atomic force microscopy and photoluminescence

* Corresponding author. E-mail: nix@vcu.edu

measurements on the coalesced ELO a-GaN sample also indicated improved material quality.

1. Introduction

In c-axis-oriented hexagonal GaN system, the spontaneous and strain-induced piezoelectric polarizations produce strong electric fields that can be somewhat advantageous for two-dimensional electron gas formation in field effect transistors (FETs) without external doping. However, these fields cause spatial separation of electrons and holes in quantum wells that are used for active regions in light emitters. Such a separation increases the recombination time[1] at the expense of the quantum efficiency,[2] and also results in a red shift of the emission, the amount of which depends on the injected carrier density due to screening. In short, additional constraints are placed on design rules in an effort to deal with polarization induced field. One approach to overcome this problem is to employ non-polar a-plane hexagonal GaN, which can be grown on r-plane sapphire using metalorganic chemical vapor deposition (MOCVD).[3,4,5] Investigations on a-plane AlGaN/GaN quantum wells[6,7,8,9] and light emitting diodes[10] have confirmed the absence of polarization-induced electric field. In order to realize high-performance nitride devices, epitaxial lateral overgrowth (ELO) method could be used to reduce the density of threading dislocations (TDs) in a-plane GaN using MOCVD.[11,12] However, one cannot overlook the wing tilt, which has been shown to introduce some complexity even for c-plane GaN ELO.[13] In this paper, we report on structural and optical characterization of a-plane GaN ELO samples grown by a two-stage MOCVD method to address the coalescence issue introduced by wing tilt.

2. Experimental procedure

The $(11\bar{2}0)$ a-plane GaN films were grown on $(1\bar{1}02)$ r-plane sapphire substrates (see ref. 5 for details). After a low-temperature GaN nucleation layer growth, a 1.5 μm-thick a-plane GaN film was deposited to be used as the subsequent ELO template. Then an approximately 100 nm-thick SiO_2 layer was grown on the a-GaN template using plasma enhanced chemical vapor deposition. Using conventional photolithography and buffer oxide etch (BOE), a striped mask pattern was transferred to SiO_2. The pattern was oriented along the $[1\bar{1}00]$ direction of GaN, consisting of 4 μm-wide open windows and 20 μm- or 10 μm-wide SiO_2 stripes, to cause the lateral growth fronts to advance along the c^+ and c^- directions. The patterned template was then reloaded into the chamber for overgrowth. Two a-GaN ELO samples were grown for this particular study, samples A and B, with TMG and NH_3 flow rates of 157 μmol/min and 3000 sccm, respectively. Sample A was grown in a single stage at 1050 ºC for 3 h while sample B was grown in two stages: at 1000 ºC for 2 h in stage I and at 1050 ºC for 3 h in stage II. Each sample contained two sections, one with 10 μm- one with 20 μm-wide stripes, grown side by side in the growth chamber. The as-grown samples were characterized by scanning electron microscopy (SEM), atomic force microscopy (AFM), x-ray diffraction (XRD), transmission electron microscopy (TEM), and low temperature photoluminescence (PL). For a better view of the overgrown layer dimensions, the SEM measurements were performed on the 20 μm stripe samples, while the rest of the analysis was focused on the 10 μm stripe samples.

3. Results and discussion

After 0.5 h of overgrowth sample A was removed from the growth chamber for investigation, and then reloaded for re-growth after cleaning using organic solvents. As seen from the SEM image in Figure 1(a), the a-GaN stripes were straight after 0.5 hours of overgrowth, with (0001) and $(000\,\bar{1})$ side walls with no other facets visible. Sample A surface was fully coalesced after a total of 3 h of growth but with striated features along and steps perpendicular to the c-axis [see Figure 1(b)]. As observed from the cross-sectional SEM image of Figure 1(c), wings with Ga-polarity are 5-6 times wider than those with N-polarity, as also verified by TEM measurements. The polarities of the two wings were determined by convergent beam electron diffraction. In addition, from the Kikuchi lines using large angle convergent beam electron diffraction (LACBED), a tilt angle of 0.25° and a twist (0.09°) between the two opposing wings were observed. As a consequence of the inherent wing tilt and largely different growth rates of the opposing wings, a clear height difference appears at the coalescence front. This height difference causes a significant surface undulation in a-plane GaN, and is the origin of steps observed in Figure 1(b).

In order to get uniform coalescence and smooth overall surface, the above-mentioned height difference should be decreased or even eliminated if possible. As shown in Figure 2, assuming the same tilt angle for both wings, if the Ga- to N-polar wing ratio is large [for example, 5:1, see Figure 2(a)], the height difference between the two opposite wings at the coalescence front will be larger than that for a smaller Ga- to N-polar wing ratio [for example, 1.6:1, see Figure 2(b)]. Therefore, in order to reduce this height difference, one needs to reduce the difference between the widths or growth rates

of the two opposite wings. Naturally, the height difference will be smaller for the samples with 10 μm-wide stripes than those with 20 μm-wide stripes.

Growth temperature is an effective parameter to control the difference in the growth rate of Ga- and N- wings. For sample B, a two-stage growth method was employed to reduce the height difference and steps associated with uneven growth rates of two opposite wings observed in sample A. During stage I, 1000 ºC growth temperature was used to enhance vertical growth while maintaining a relatively lower lateral growth rate which is not drastically different for the Ga- and N-fronts at this temperature. Figure 3(a) shows that, after stage I growth, the sidewalls of a-GaN stripes were composed of $\{11\bar{2}2\}$ facets rather than (0001) or $(000\bar{1})$. It is worth pointing out that a large portion of the lateral growth was established in stage I where the Ga- to N- polar wing width ratio is close to 1. At stage I there is no coalescence between two wings grown laterally with the opposite polarity. After 2 h of growth in stage I, temperature was elevated to 1050 ºC to enhance the lateral growth of a-GaN for complete coalescence. Figure 3(b) and Figure 3(c) show the plan-view and cross-sectional SEM images, respectively, for sample B after full coalescence (~ 15 μm total thickness). The Ga-polar wing is around 1.6 times wider than the N-polar wing. Although Ga-wing still had a larger growth rate than the N-wing in stage II, the difference in average growth rates (averaged over stage I and stage II) between these two wings has been greatly reduced. The surface undulations in sample B were much smaller than those observed in sample A, and the two neighboring wings in sample B were almost at the same height at the meeting front. During stage II growth, with the temperature elevated, the sidewalls became relatively vertical. After coalescence is taking place voids are overgrown. These results indicate that the attempts to suppress

the uneven average growth rates of Ga- and N- wings by enhancing the vertical growth rate in the early stage of the growth were successful.

XRD measurements were carried out on both samples using a Phillips X'pert MRD system to determine the wing tilt angles. Wing tilt has been defined in the conventional c-plane GaN ELO as the tilt between the overgrown wings and the window plane, and can be obtained by measuring XRD rocking curves with the incident x-ray beam perpendicular to the SiO_2 stripes. For comparison, XRD rocking curve scans were carried out with three different ϕ angles which is the angle of rotation about the sample surface normal, and is defined as 0° when the projection of incident x-ray beam is parallel to the SiO_2 mask stripes. As shown in Figure 4, for ϕ=0°, only one diffraction peak from a-plane of GaN can be observed, with a full width at half maximum (FWHM) of 0.40º and 0.19º for samples A and B, respectively. For ϕ=90º (x-ray beam is perpendicular to the mask stripes), sample A and B exhibit two and three peaks, respectively, the orders of which are reversed for ϕ=270º. The strong peak observed for sample A is from the Ga-polar wings, since the width of the Ga-wing is 5-6 times larger than that of the N-wing as verified by SEM images discussed above. Similarly, the window width (4 μm) is also smaller than that of the Ga-wings. Therefore, the weak peak is assumed to be from the windows and/or N-wings, and the observed tilt angle of 0.86º is anticipated considering the relatively large width of the Ga-wings. Similarly for sample B [Figure 4(b)], the strongest peak is from Ga-polar wings, while the central one is from the crystal plane in windows, and third is from the N-polar wings. In the case of sample B, smaller XRD linewidth compared to that for sample A indicates improved crystalline quality, and therefore, peaks from all three regions are distinguishable. By fitting the rocking curve

for ϕ=90^{o} with three Gaussian peaks, the wing tilts for Ga- and N- polar wings are determined to be 0.44^{o} and 0.37^{o}, respectively, with a total tilt angle of 0.81^{o} between the two wings. The tilt angle values obtained from XRD are more than three times larger than that obtained from the LACBED. This large variation may be attributed to the locality of the LACBED measurement, while XRD provides a value averaged over a much larger area.

Extended defect densities in samples A and B were also measured by TEM. The TD density was reduced from 4.2×10^{10} cm^{-2} in the windows to 1.0×10^{8} cm^{-2} in the wings for sample A. However, a relatively high density of basal stacking faults (BSFs), 1.2×10^{4} cm^{-1}, was still observed in the wing areas compared to 1.3×10^{6} cm^{-1} in the windows. [14] Formation of BSFs is not surprising since they have the lowest formation energy. [15] The most important is that these stacking faults propagate to the sample surface, therefore they will intersect any active area of the device grown on such substrtaes. For the overgrowth of the layers grown along polar direction BSFs are formed only close to the substrate. [16] In the upper part of the layer that BSFs were rarely observed.[17] As shown in Figure 5(b) dislocations were also found at the meeting fronts, as in the case of c-plane ELO.[18] Sample B also showed a similar reduction of dislocations in the wings [Figure 5(c)]. The TD density was reduced by almost two orders of magnitude in the wings. However, when these wings coalesce a grain boundary is formed on the prismatic plane with the shift vector parallel to (0001) (Fig. 5c). These boundaries sometime eliminate BSFs propagating from the substrate, but often they are source of new defects propagating to the surface. Nevertheless, sample B differed from sample A in that the

wings with Ga-polarity were only 1.5-2.0 times wider than those with N-polarity and also the surface was much smoother in the former.

Tapping-mode AFM measurements revealed significantly different densities of surface pits in the window and wing regions of the as grown samples. These might be prismatic stacking faults terminated by dislocations. [19] Figure 5(d) shows the AFM image near the window-N-wing boundary for sample B. For sample B, the pit density in the windows (~3.0×10^{9} cm^{-2}) was around two orders of magnitude larger than that in the wings (~3.7×10^{7} cm^{-2}). TEM and AFM results therefore confirm the effective defect reduction in a-plane ELO GaN with mask pattern along $[1\,\bar{1}00]$ of GaN.

It is commonly observed that growth rate on Ga- and N-polar surface is different, but an origin of this difference is not well established. This behavior has also been observed in the lateral overgrowth of m-plane GaN.[20] Some authors tentatively attributed it to different adsorption or desorption rates on Ga- and N- faces. However, our experiments show that under the same conditions N-face and Ga-face c-plane GaN have similar growth rates, which was also verified by others.[21] Therefore, we speculate that this phenomenon may be related to differences in chemical stability of Ga- and N-faces since the latter has been shown to be less resistive to wet chemical etching.[22] During the growth of a-GaN, relatively lower amount of ammonia and higher growth temperature in hydrogen atmosphere may make N-face even less stable than the Ga-face, thereby inducing a smaller growth rate for the N-face GaN.

For further evaluation of the material quality, low temperature PL was performed on the overgrown GaN layers using 325 nm excitation from a HeCd laser. Figure 6(a) shows the PL spectra at 15 K for sample B. The near bandedge emission is composed of

two peaks at 3.475 and 3.419 eV. The 3.475 eV peak, which has a FWHM value of 19 meV, most probably is a combination of the free exciton and donor bound exciton transitions. The band edge emission in sample B was around two orders of magnitude stronger than that in a control sample grown directly on sapphire without the ELO pattern but under similar growth conditions [see also Figure 6(a)]. As shown in Figure 6(b), the main bandedge peak slightly blueshifts with increasing temperature up to 50 K and then starts to redshift reaching 3.415 eV at 300 K. This blueshift up to 50 K is due to the dissociation of the bound exciton with increasing thermal energy which makes the free exciton peak to dominate. Because both the donor bound exciton and free exciton transitions are broad, it is not possible to delineate them even at 15 K. The peak at 3.419 eV for the 15 K PL is most probably due to recombination of carriers/excitons bound to stacking faults,[23] which are common in a-GaN as verified by the TEM results discussed above. This peak has also been attributed to the recombination of excitons bound to structural defects on the surface.[24] The blue and yellow emission bands, which are characteristic to GaN, are also observed with peaks around 2.96 and 2.25 eV, respectively. The blue band quenches above 150 K and the maximum intensity of the yellow band remains almost the same up to 300 K. At room temperature, the band edge luminescence is more than two orders of magnitude weaker than the yellow luminescence, indicating that further improvements of the a-plane GaN quality are necessary.

4. Conclusions

Epitaxial lateral overgrowth of a-plane GaN is more challenging than that of c-plane GaN due to the different growth polarities of two opposite wings. This different

growth polarities lead to different growth rate in different crystallographic directions, e.g. laterally and vertically, leading to different wing heights and difficulty of wing coalescence. In order to obtain flat surface one needs to reduce the wing height difference and bring to wing coalescence. For this purpose two-stage growth was applied. Initially we tried to enhance vertical growth and then we applied an elevated temperature to enhance the lateral growth rate. However, TEM studies indicate formation of a new boundary on inclined prismatic plane at the area where two wings coalesced due to formation of step height between wo wings. Dislocations were also formed along vertical a-growth direction. Despite of this we can show that threading dislocation density was reduced from $4.2\times10^{10}cm^{-2}$ in the window regions to $1.0\times10^{8}cm^{-2}$ in the wing regions, and that relatively high density of basal stacking faults of $1.2\times10^{4}\ cm^{-1}$ was present in the wings. The improvement in the overgrown layer quality by ELO was also verified by AFM, which showed reduced surface pit density in the wings of the as grown samples and by PL in terms of increased intensity of the bandedge emission.

This work in both laboratories is supported by the Air Force Office of Scientific Research under the direction of Dr. K. Reinhardt. The use of NCEM facility in Berkely is appreciated. Useful discussions with C. J. Moore and V. P. Kasliwal are acknowledged.

Error!

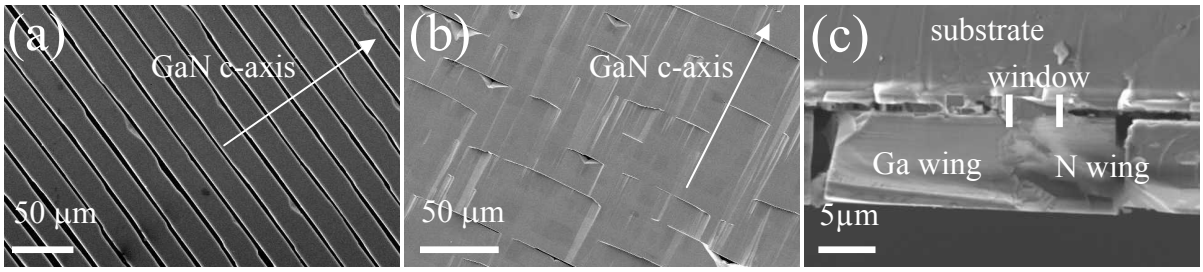

Figure 1: Plan-view SEM images for sample A after (a) 0.5 h and (b) 3.0 h of growth.(c) Cross-sectional SEM image for sample A after 3 h of growth.

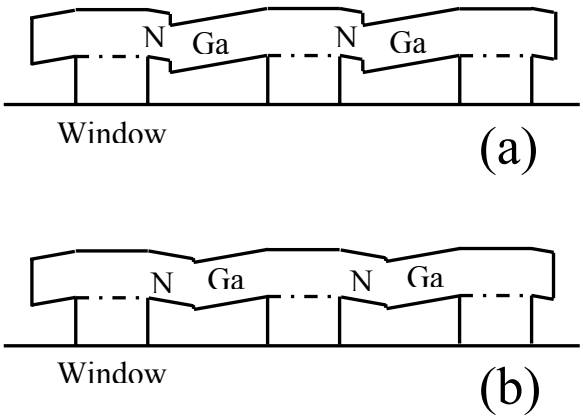

Figure 2: Schematics for a-plane GaN ELO showing the origin of the height difference between two neighboring wings (not in exact proportion), with Ga- to N- polar wing width ratio of (a) 5:1, (b) 1.6:1. The larger this ratio is, the larger the height difference between the two opposite wings at the coalescence fronts.

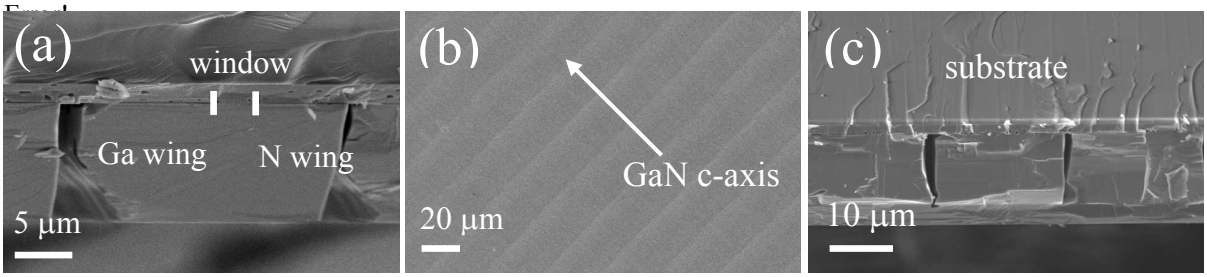

Figure 3: (a) Cross-sectional SEM image for sample B after 2 h of growth at 1000^{o}C. (b) & (c) plan-view and cross-sectional SEM images for sample B, after a total of 5 h of growth.

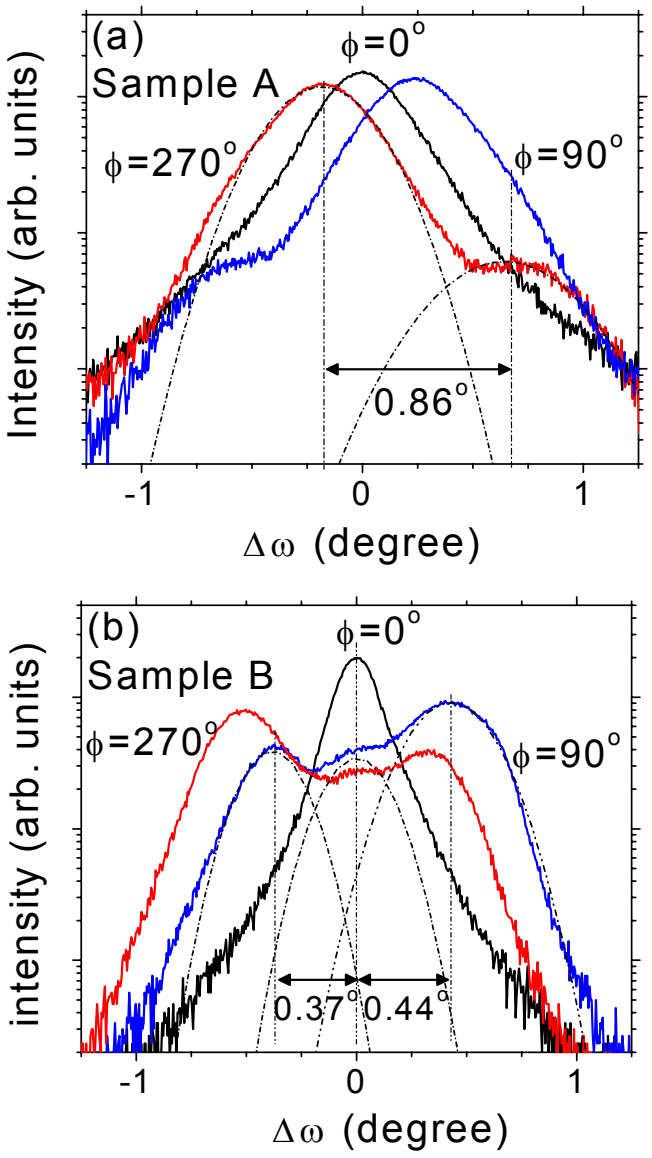

Figure 4: XRD omega scan for (a) sample A and (b) sample B with different ϕ angles. The ϕ angle is the angle of rotation about the sample surface normal, and is defined as 0º when the projection of incident x-ray beam is parallel to the SiO_2 stripes of mask. The dashed lines in the figures correspond to the multiple Gaussian fits to the rocking curve data with ϕ=90º.

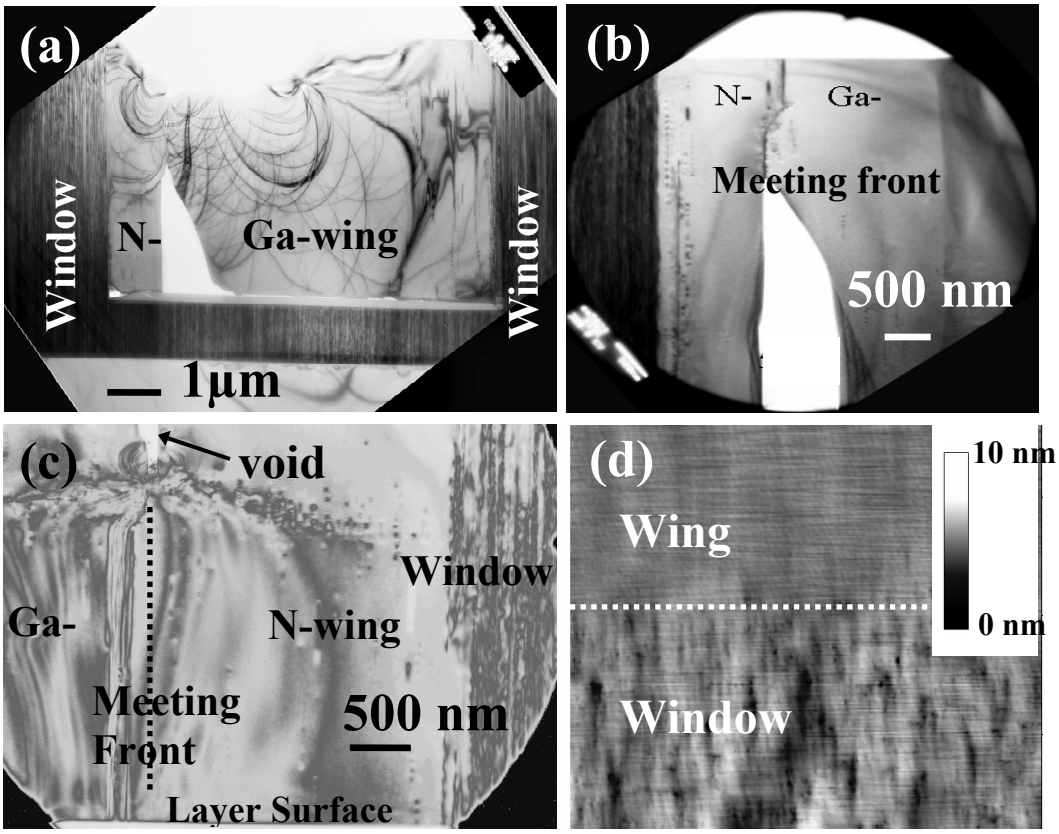

Figure 5: (a) Cross-sectional TEM image for sample A showing the window and wing regions. (b) Cross-sectional TEM image for sample A showing the meeting front between Ga- and N- wings. (c) Cross-sectional TEM image for sample B showing the meeting front, Ga- and N- wings as well as the window region. (d) $4\times4\mu m^2$ AFM image near the window-N-wing boundary of sample B, showing different surface pit densities for the window and the wing.

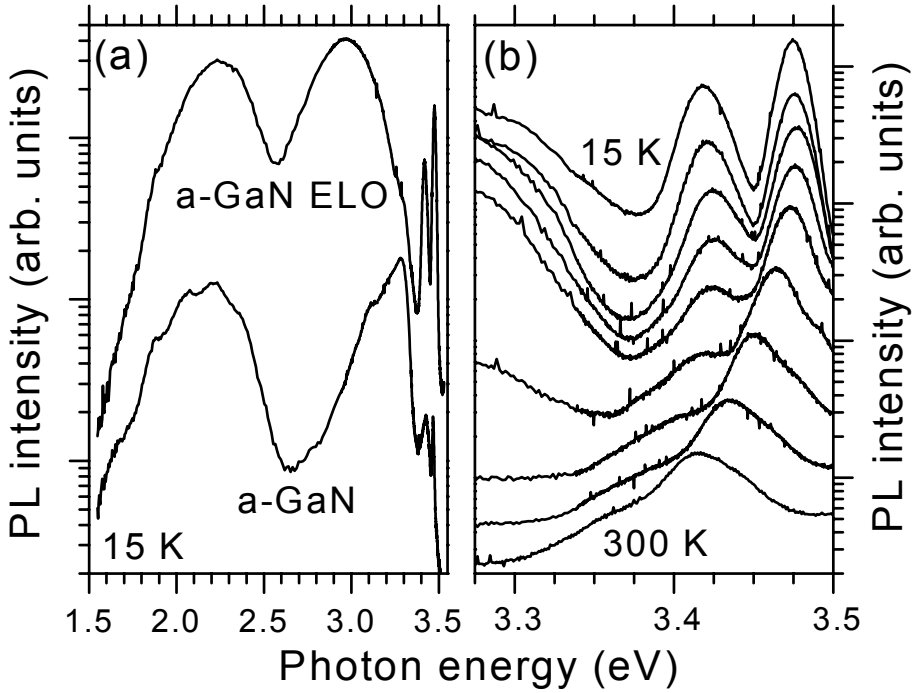

Figure 6: (a) 15 K photoluminescence spectra for sample B (a-GaN ELO) and a regular a-plane GaN sample (a-GaN) grown without the ELO pattern but under similar conditions. (b) PL spectra for sample B at temperatures 15, 25, 50, 75, 100, 150, 200, 250, and 300 K (from top to bottom and vertically shifted for clarity).

References:

[1] R. Langer, J. Simon, V. Ortiz, N. T. Pelekanos, A. Barski, R. Andre, and M. Godlewski, Appl. Phys. Lett **74**, 3827 (1999).

[2] T. Deguchi, K. Sekiguchi, A. Nakamura, T. Sota, R. Matsuo, S. Chichibu, and S. Nakamura, Jpn. J. Appl. Phys. **38**, L914 (1999).

[3] H. M. Ng, Appl. Phys. Lett. **80**, 4369 (2002).

[4] M. D. Craven, S. H. Lim, F. Wu, J. S. Speck, and S. P. DenBaars, Appl. Phys. Lett. **81**, 469 (2002).

[5] X. Ni, Y. Fu, Y. T. Moon, N. Biyikli, H. Morkoç, J. Cryst. Growth **290**, 166 (2006).

[6] H. M. Ng, A. Bell and F. A. Ponce, S. N. G. Chu, Appl. Phys. Lett. **83**, 653 (2003).

[7] T. Koida, S. F. Chichibu, T. Sota, M. D. Craven, B. A. Haskell, J. S. Speck, S. P. DenBaars, and S. Nakamura, Appl. Phys. Lett. **84**, 3768 (2004).

[8] H. Teisseyre, C. Skierbiszewski, B. Łucznik, G. Kamler, A. Feduniewicz, M. Siekacz, T. Suski, P. Perlin, I. Grzegory, and S. Porowski, Appl. Phys. Lett. **86**, 162112 (2005)

[9] S. Porowski, I. Grzegory, B.Łucznik, B. Pastuszka, M. Boćkowski, H. Teisseyre, Cz. Skierbiszewski, G. Kamler, G. Nowak, J. Smalc and M. Kryśko, Proc. of SPIE Opto 06 January 22-25 2006 San Jose CA.

[10] A. Chitnis, C. Chen, V. Adivarahan, M. Shatalov, E. Kuokstis, V. Mandavilli, J. Yang, and M. A. Khan, Appl. Phys. Lett. **84**, 3663 (2004).

[11] M. D. Craven, S. H. Lim, F. Wu, J. S. Speck, and S. P. DenBaars, Appl. Phys. Lett. **81**, 1201 (2002).

[12] C. Chen, J. Yang, H. Wang, J. Zhang, V. Adivarahan, M. Gaevski, E. Kuokstis, Z. Gong, M. Su and M. A. Khan, Jpn. J. Appl. Phys. **42**, L640 (2003).

[13] P. Fini, H. Marchand, J. P. Ibbetson, S. P. DenBaars, U. K. Mishra, J. S. Speck, J. Cryst. Growth. **209**, 581 (2000).

[14] Z. Liliental-Weber, D. Zakharov, B. Wagner, and R.F. Davis, Proceedings of the SPIE (2005).

[15] D. Hull and D.J. Bacon, *Introduction to Dislocation* (Pergamon Press, Oxford, 1984).

[16] Z. Liliental-Weber, D. Cherns, J. Appl. Phys. **89**, 7833 (2001).

[17] F. A. Ponce, Mater. Res. Bull. **22**, 51 (1997).

[18] Z. L. Weber, M. Benamara, W. Swider, J. Washburn, J. Park, P. A. Grudowski, C. J. Eiting, R. D. Dupuis, MRS Internet J. Nitride Semicond. Res. **4S1**, G4.6 (2000).

[19] D.N. Zakharov, Z.Liliental-Weber, B. Wagner, Z. J. Reitmeier, E. A. Preble, and R. F. Davis. Phys. Rev. **B 71**, 235334-42 (2005).

[20] B. A. Haskell, T. J. Baker, M. B. McLaurin, F. Wu, P. T. Fini, S. P. DenBaars, J. S. Speck, and S. Nakamura, Appl. Phys. Lett. **86**, 111917 (2005).

[21] R. Collazo, S. Mita, A. Aleksov, R. Schlesser, and Z. Sitar, J. Cryst. Growth. **287**, 586 (2006).

[22] Y. Gao, M. D. Craven, J. S. Speck, S. P. DenBaars, and E. L. Hu, Appl. Phys. Lett. **84**, 3322 (2004).

[23] P. P. Paskov, R. Schifano, T. Paskova, T. Malinauskas, J.P. Bergman, B. Monemar, S. Figge, and D. Hommel, Physica B **376–377**, 473 (2006).

[24] M. A. Reshchikov and H. Morkoç, J. Appl. Phys. **97**, 061301 (2005).